

A new silver cluster that emits bright-blue phosphorescence

Supplementary Information

Jin-Sen Yang,^a Miao-Miao Zhang,^a Zhen Han,^a Hai-Yang Li,^a Lin-Ke Li,^a Xi-Yan Dong,^{*ab}
Shuang-Quan Zang,^{*a} and Thomas C. W. Mak^c

^a*Green Catalysis Center, and College of Chemistry, Zhengzhou University, Zhengzhou
450001, China*

^b*College of Chemistry and Chemical Engineering, Henan Polytechnic University,
Jiaozuo 454000, China.*

^c*Department of Chemistry, The Chinese University of Hong Kong, Shatin, New
Territories, Hong Kong SAR. China.*

*E-mail: zangsqzg@zzu.edu.cn (S-Q Zang); dongxiyan0720@hpu.edu.cn (X-Y Dong);

Materials and Methods

Materials and Reagents

All chemicals and solvents obtained from suppliers were used without further purification. All solvents were analytical grade reagent.

Instrumentation.

Powder X-ray diffraction (PXRD) patterns of **NC-Ag6** were collected at room temperature in air using an X'Pert PRO diffractometer (Cu-K α). Fourier transform infrared (FT-IR) spectra were recorded on a Bruker TENSOR 27 FT-IR spectrometer in the 400-4000 cm⁻¹ region with KBr pellets. Thermogravimetry analyses (TGA) were performed on a TA Q50 system under a N₂ atmosphere (flow rate = 60 mL·min⁻¹) in the temperature range 30-600 °C at a heating rate of 10 °C min⁻¹. ¹H nuclear magnetic resonance (NMR) spectra were recorded at RT on a Bruker 400 spectrometer; the samples of **NC-Ag6** solvents for ¹H NMR were dissolved in deuterated dimethyl sulfoxide and **dpppy** solvents for ¹H NMR were dissolved in deuterated chloroform, both containing TMS as an internal standard. Mass spectra (MS) were recorded on a X500R QTOF spectrometer. Elemental analyses (EA) were carried out with a Perkin-Elmer 240 elemental analyzer. UV-Vis absorption spectra were recorded using a Hitachi UH4150 UV-Visible spectrophotometer in the range 200-800 nm. UV-visible diffuse reflectance spectra of samples were recorded at room temperature in the range of 250-800 nm using a UH4150 spectrophotometer equipped with an integrating sphere.

X-Ray Crystallography

Single-crystal X-ray diffraction measurement of compound **NC-Ag6** was performed on a Rigaku XtaLAB Pro diffractometer. Data collection and reduction were performed using the program CrysAlisPro.¹ The structure was solved with direct methods (*SHELXS*)² and refined by full-matrix least squares on *F*² using *OLEX2*,³ which utilizes the *SHELXL-2015* module.⁴ All the atoms were refined anisotropically. Hydrogen atoms were placed in calculated positions refined using idealized geometries and assigned fixed isotropic displacement parameters. Structure refinement was handled with different strategies according to the electron density distribution. The detailed information of the crystal data, data collection and refinement results for the compounds are summarized in Tables of crystal data and structure refinements.

DFT calculations

The density functional theory (DFT) and time-dependent density functional theory (TD-DFT) calculations were performed with Gaussian 09 using B3LYP functional. All calculations were conducted using 6-31G* basis set for H, C, N, O, F and P atoms, and LanL2DZ effective core potentials for Ag atoms. The single crystal structure was chosen as the initial guess for ground state optimization. Then, frequency calculations at the same level of theory were carried out to identify all of the stationary points as minima (zero imaginary frequency). The calculated absorption spectra were obtained from GaussSum 2.1. Hirshfeld population analysis was conducted by Multiwfn 3.4.

Synthesis of [Ag-SCH₂CH₂-C₆H₅]_n complex

First, AgNO₃ (3 mmol) was completely dissolved in 20 mL of acetonitrile (MeCN) by sonication, then, 2-Phenylethanethiol (3 mmol) was added. Next, Triethylamine (1 mmol) was added quickly to the reaction. The reaction was continued at room temperature (RT) in the dark overnight. The next day, the sample was centrifuged at 8000 rpm for 5 min give a white precipitate, which was washed at least 5 times with ethanol (CH₃CH₂OH).

Synthesis and purification of Ag₆(dpppy)₂(CF₃COO)₆

150 mg of **dpppy** was dissolved in 40 mL chloroform (CHCl₃). Then 220 mg of silver trifluoroacetate (CF₃COOAg) was added. After stirring for 20 minutes at room temperature, the product was precipitated and collected through filtration, followed by washed with chloroform and water several times to remove excess **dpppy** and CF₃COOAg. The yield of **NC-Ag6** was 40% (in silver atom basis). Elemental analysis (%) for evacuated **NC-Ag6** (C₇₀H₄₆Ag₆F₁₈N₂O₁₂P₄): calcd. C 37.87, H 2.09, N 1.26; found C 38.54, H 2.28, N 0.91; The single crystal was obtained by the following method:

5 mg [Ag-SCH₂CH₂-C₆H₅]_n was added into 4 mL CHCl₃, then 20 mg CF₃COOAg was added. After stirring for 1 minute, the colorless clear liquid was obtained. Then 10 mg **dpppy** ligand was added. After stirring for 5 minutes and then filter, the filtrate was then allowed to evaporate slowly at RT in the dark under ambient conditions. After three days, colorless crystals were obtained.

Film Preparation

Firstly, **NC-Ag6** and YAG : Ce³⁺ mixture in a certain proportion (1 : 1) was added into polymethyl methacrylate dichloride solution, and stirred until completely well-distributed. Finally, the mixed solution was dropped on a glass template by spread, evaporation and solidification to form film.

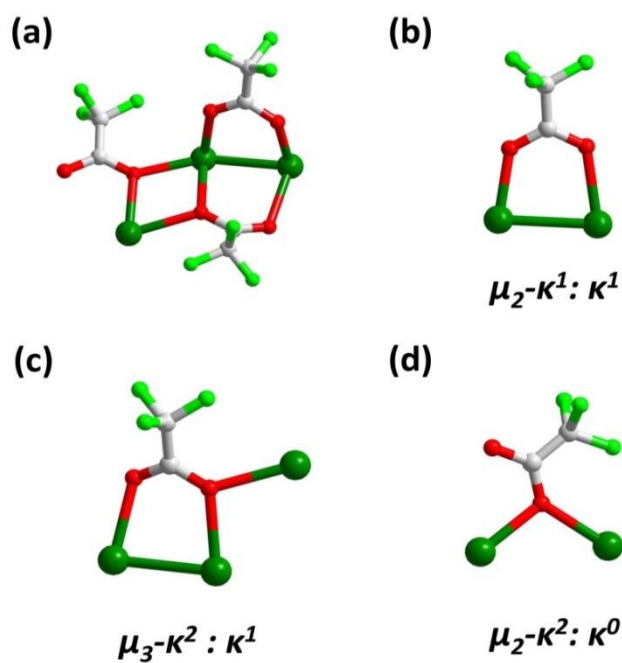


Figure S1. The three coordination modes of CF_3COO^- with silver ions. Color code: Ag, green; F, cyan; C, gray; O, red.

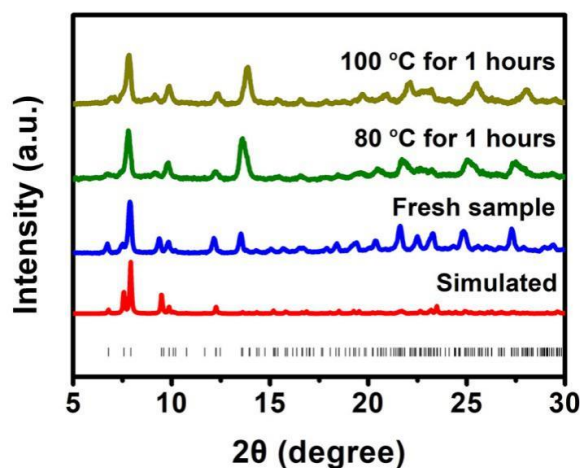


Figure S2. The experimental and simulated PXRD spectra of NC-Ag6.

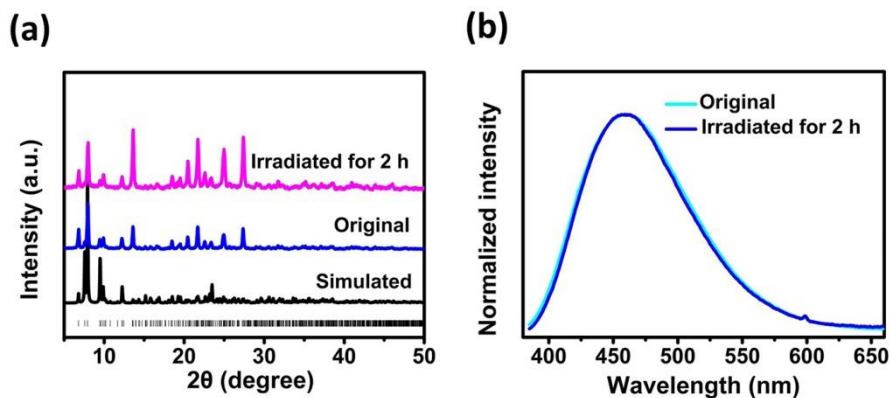


Figure S3. The PXRD (a) and emission spectra (b) of NC-Ag6 before and after irradiation by xenon lamp (power : 300W) .

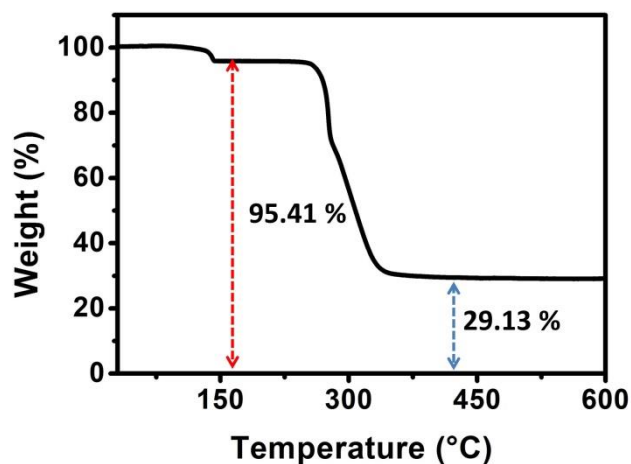


Figure S4. The thermal gravimetric curve of **NC-Ag6**. The first weight loss (4.59 %) from room temperature to 140 °C could be ascribed to the removal of one CF_3COO^- (calcd 4.55 %), The weight loss (70.87 %) between 280 °C and 600 °C should be caused by the ligands complete dissociation (calcd 70.85 %).

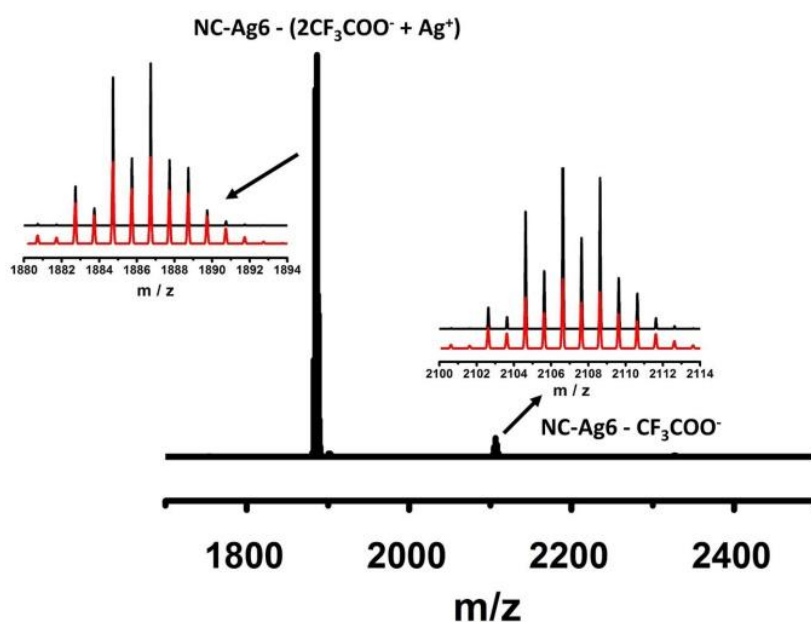


Figure S5. Positive mode ESI MS of complex in DMF, inset: overlap of the experimental data (black) and the simulated spectrum (red). The parent $[\text{NC-Ag6}]^+$ ion was not detected, presumably owing to the lability of the coordinated trifluoroacetate in the gas phase. The spectrum showed a signal at m/z 2106.6151 which corresponds to the $[\text{NC-Ag6} - \text{CF}_3\text{COO}^-]^+$ ion (calcd m/z 2106.6166), and a major signal at m/z 1886.7234 in its ESI mass spectrum, which corresponds to the $[\text{NC-Ag6} - (2\text{CF}_3\text{COO}^- + \text{Ag}^+)]^+$ ion (calcd m/z 1886.7267).



Figure S6. Photograph of crystalline powder of **NC-Ag6**. Left: under ambient light. Right: under UV light of 365 nm.

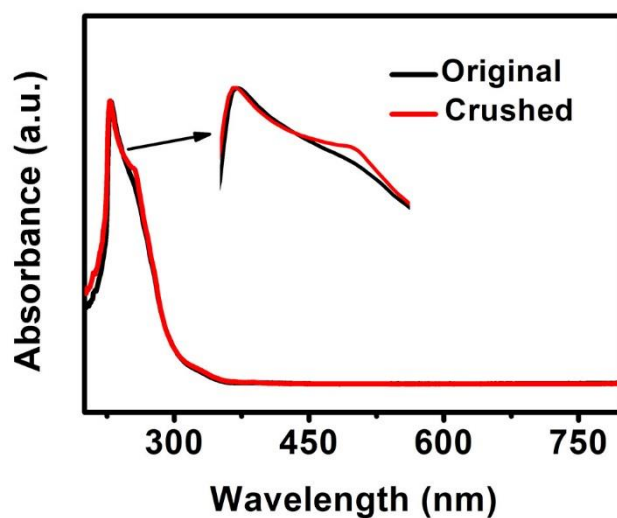


Figure S7. The UV-vis absorption spectra of **NC-Ag6** original and crushed in dichloromethane. Insert: partial enlarged drawing.

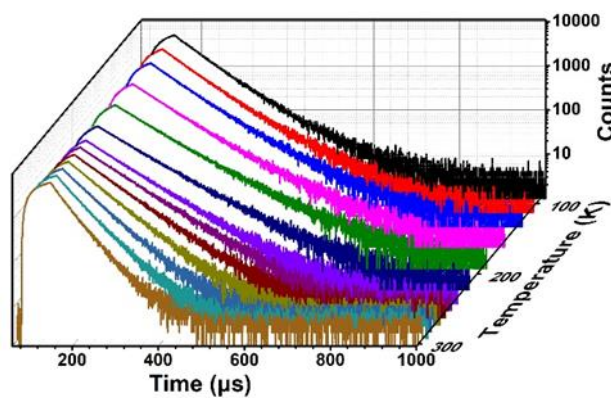


Figure S8. The temperature-dependent emission lifetime of **NC-Ag6** at $\lambda_{em}=453$ nm at room temperature.

Table S1. Luminescence properties of **dpppy** and **NC-Ag6** (τ : emission lifetime, Φ : emission quantum yield).

	λ_{\max} (nm)	τ (μs)	Φ (%)
dpppy	420	0.75×10^{-3}	4.12
NC-Ag6 crystals	453	22.4	22.4

Table S2 Temperature-dependent emission lifetime and corresponding fractional contributions (%) of solid-state **NC-Ag6** excited at 355 nm, respectively (χ^2 : fitting parameter).

Temperature	χ^2	τ_1 (μs) (%)	τ_2 (μs) (%)	τ (μs)
83K	0.97	108 (17.46)	57.7 (82.54)	66.5
103K	0.97	56.1 (73.32)	97.9 (26.68)	67.3
123K	0.98	111 (17.54)	61.1 (82.49)	69.8
153K	1.01	60.8 (66.31)	97.9 (33.69)	73.3
183K	0.99	63.6 (58.5)	91.5 (41.5)	78.3
213K	1.02	64.0 (47.23)	91.5 (52.77)	78.5
233K	1.03	110 (8.51)	69.0 (91.49)	72.4
243K	0.97	51.3 (14.5)	72.7 (85.5)	69.6
253K	0.98	60.8 (92.33)	92.1 (7.67)	63.2
263K	1.02	99.2 (4.24)	53.7 (95.76)	55.6
273K	1.07	35.1 (18.94)	52.5 (81.06)	49.2
283K	1.06	28.4 (22.97)	46.7 (77.03)	42.5
293K	1.10	25.5 (30.35)	41.4 (69.65)	36.3

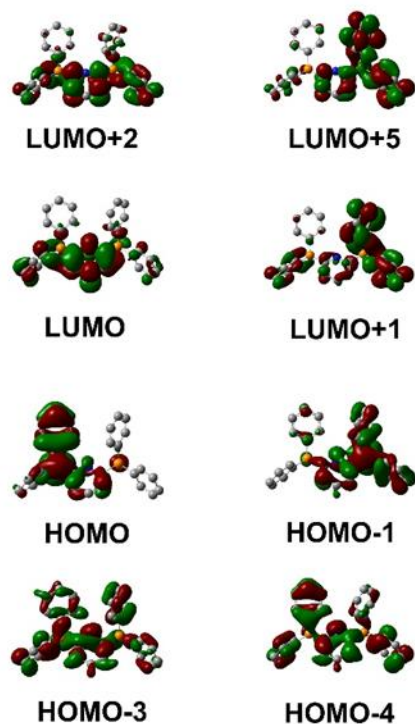


Figure S9. Selected frontier molecular orbitals representations for **dppy**. Detailed orbital compositions were listed in Table S3.

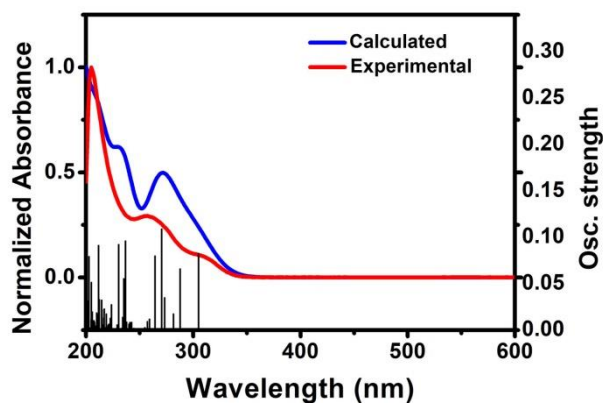


Figure S10. The calculated spectrum of **dppy** (blue) compared to the experimental UV-vis absorption spectrum (red). The band centered at 304 nm was attributed to HOMO \rightarrow LUMO with 95% contribution. The band at 271 nm mainly originated from the HOMO-1 \rightarrow LUMO+1 (56%), HOMO \rightarrow LUMO+1 (15%) and HOMO-1 \rightarrow LUMO+2 (15%). Black bars showed the individual transitions (delta-function-like peaks showing the relative oscillator strengths).

Table S3. Hirshfeld percentage (B3LYP/(LanL2DZ/6-31G*) level) of orbital compositions of frontier molecular orbitals in **dpppy** and energy level. D refers to two $-PPh_2$ groups. A refers to the fragment of pyridine rings. (H = HOMO, L = LUMO).

	D	A	
Orb#	Composition	Composition	Energy/eV
H-5	90.16	3.23%	-7.17854
H-4	57.88%	37.15%	-7.05963
H-3	55.36%	39.79%	-7.00358
H-2	93.53%	0.42%	-6.78128
H-1	77.24%	19.2%	-6.13531
HOMO	81.10%	15.48%	-5.85287
LUMO	30.88%	63.89%	-0.84433
L+1	84.93%	8.25%	-0.53631
L+2	44.39%	49.62%	-0.51753
L+3	72.93%	20.13%	-0.3804
L+4	88.54%	1.76%	-0.0751
L+5	76.45%	16.31%	-0.03211

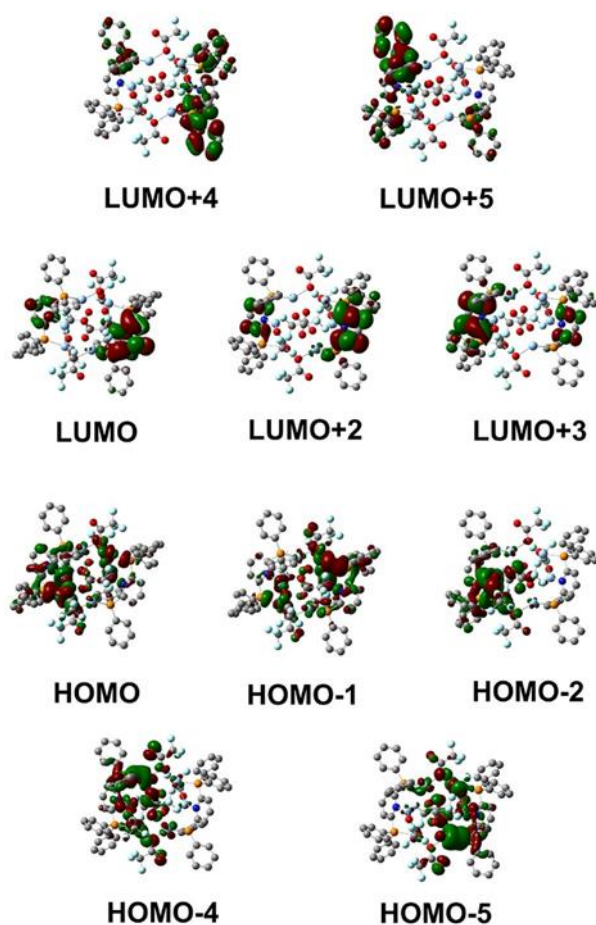


Figure S11. Selected frontier molecular orbitals representations for **NC-Ag6**. Detailed orbital compositions were listed in Table S4.

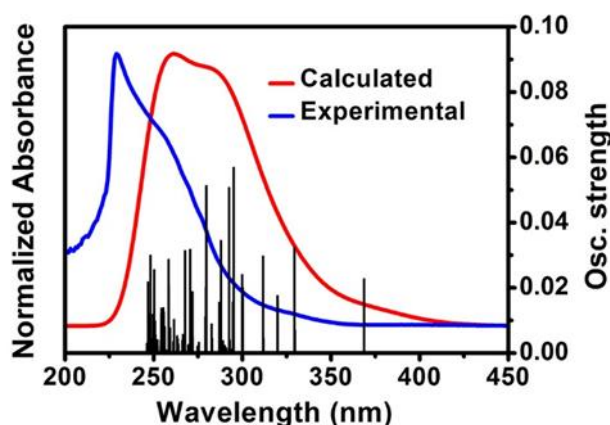


Figure S12. The calculated spectrum of **NC-Ag6** (red) compared to the experimental UV-vis absorption spectrum (blue). The band centered at 295 nm mainly originated from the HOMO \rightarrow LUMO+5 (27%), HOMO-1 \rightarrow LUMO (14%) and HOMO-2 \rightarrow LUMO (14%). The band at 279 nm mainly originated from the HOMO-4 \rightarrow LUMO+3 (40%) and HOMO-5 \rightarrow LUMO+2 (28%). Black bars showed the individual transitions (delta-function-like peaks showing the relative oscillator strengths). The gap between the calculated and the experimental value may be related to the interactions between either nanoclusters or nanoclusters and solvent molecules.^{5,6}

Table S4. Hirshfeld percentage (B3LYP/(LanL2DZ/6-31G*) level) of orbital compositions of frontier molecular orbitals in **NC-Ag6** and energy level. Ag refers to all six silver atoms. O, P and N refer to the atoms of six CF₃COO⁻ groups and two **dpppy**, respectively. (H = HOMO, L = LUMO).

	Ag	O	P	Py	Ph	
Orb#	Composition	Composition	Composition	Composition	Composition	Energy/eV
H-5	37.49%	29.39%	8.95%	3.96%	10.98%	-6.8109351
H-4	37.65%	33.78%	7.58%	3.23%	8.92%	-6.7064487
H-3	37.73%	33.09%	4.42%	6.16%	11.21%	-6.5889015
H-2	38.00%	33.19%	4.28%	5.88%	11.44%	-6.5804664
H-1	44.36%	37.62%	11.29%	9.55%	11.36%	-6.2357157
HOMO	44.98%	16.20%	11.24%	7.41%	11.44%	-6.214764
LUMO	4.65%	0.67%	7.05%	73.32%	8.5%	-1.9354473
L+1	4.46%	0.63%	0.71%	93.25%	16.6%	-1.9253796
L+2	4.16%	0.65%	0.89%	66.56%	13.2%	-1.5109713
L+3	4.12%	0.65%	8.93%	57.99%	21.86%	-1.5009036
L+4	4.60%	0.83%	11.56%	6.97%	69.45%	-1.2176475
L+5	4.21%	0.75%	11.23%	9.48%	67.69%	-1.210845

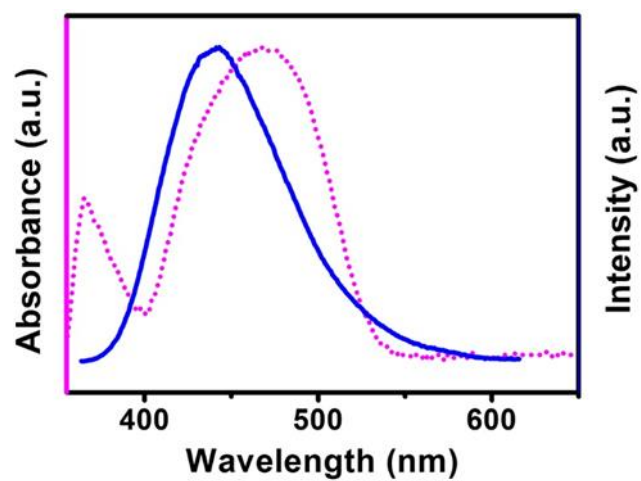


Figure S13 UV-vis diffuse reflectance spectrum of YAG : Ce³⁺ (purple dash line) and emission spectrum of **NC-Ag6** (blue solid line) in solid-state.

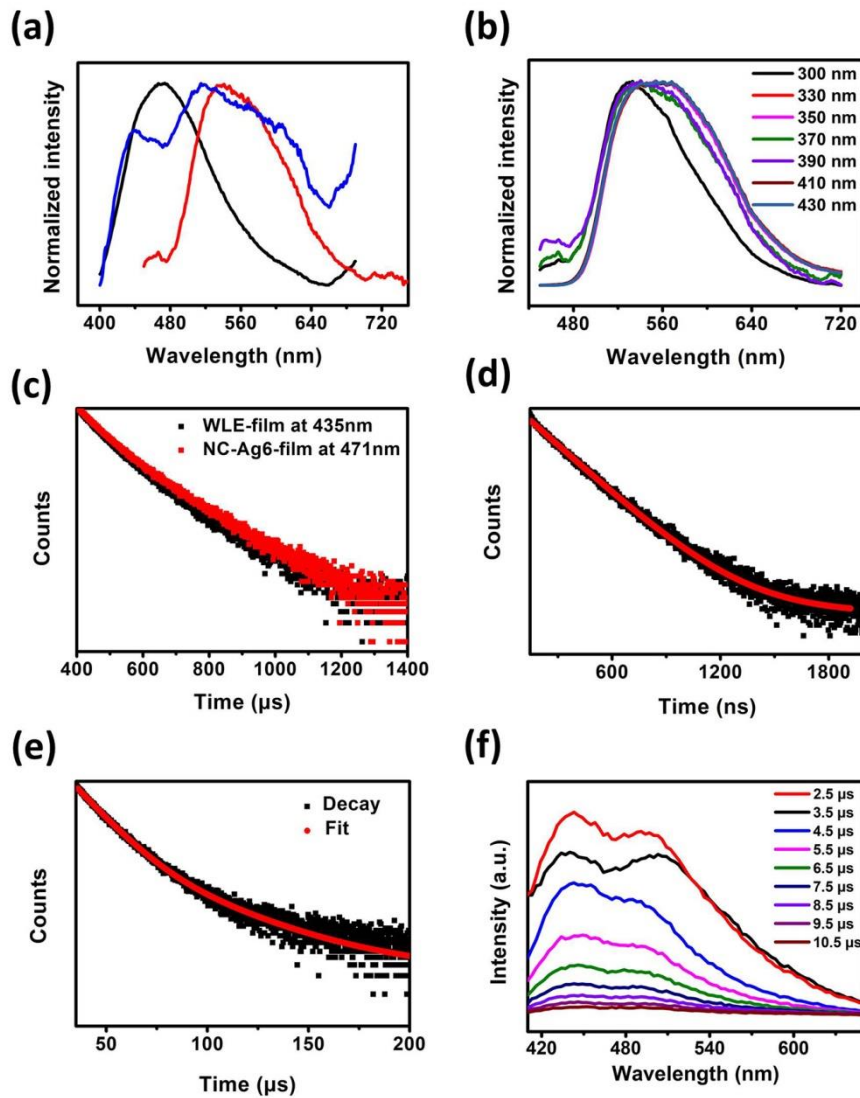


Figure S14 (a) Normalized emission spectra of **NC-Ag6** film (black line), WLE film (blue line) and YAG : Ce³⁺ film (red line) excited at 370 nm. (b) Emission spectra of YAG : Ce³⁺ film at the different excitation wavelengths. (c) RT time-resolved emission decays spectra of WLE film at 435 nm and **NC-Ag6** film at 471 nm, d) RT time-resolved emission decays spectra of YAG : Ce³⁺ film at 540 nm and (e) WLE film at 512 nm. (f) Time resolved emission spectra of WLE film excited at 355 nm. Emission Lifetime: WLE film at 435 nm was 16.85 μs, WLE film at 512 nm was 14.79 μs, YAG : Ce³⁺ at 540 nm was 63.94 ns and **NC-Ag6** film at 471 nm was 18.49 μs.

Förster resonance energy transfer efficiency E was determined from the emission lifetime of donor molecule as follows:

$$E = 1 - [\tau_{DA}/\tau_D] \quad (\text{equation 1})$$

where τ_D is the emission lifetime of donor in absence of acceptor and τ_{DA} is the emission lifetime of donor in presence of acceptor. Here, τ_D is the emission lifetime of **NC-Ag6** film at 471nm, τ_{DA} is the emission lifetime of WLE film at 435 nm. E was calculated as 9%.

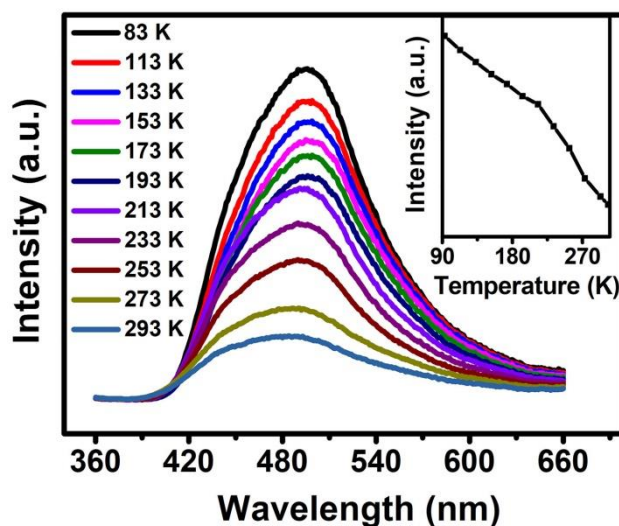


Figure S15. Temperature dependence of luminescence spectra of **NC-Ag6** after grinding at excitation wavelength of 365 nm. The insert showed temperature-dependence of the emission intensity.

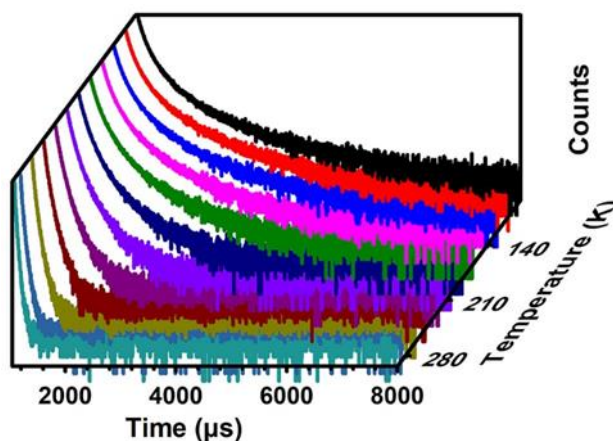


Figure S16. The temperature-dependent emission lifetime spectra of **NC-Ag6** after grinding at $\lambda_{em}=493$ nm.

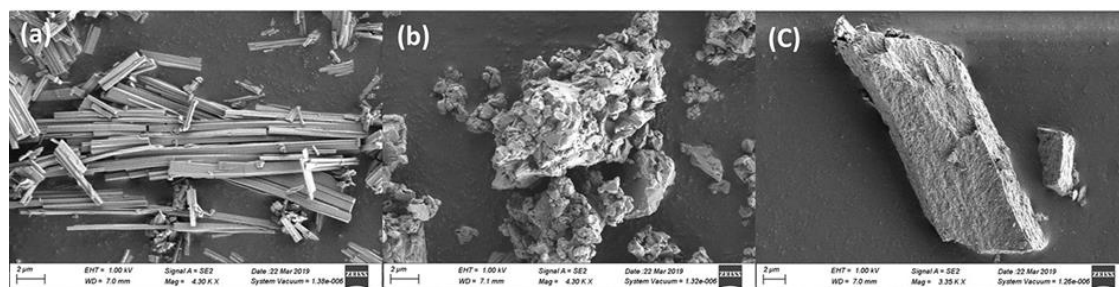


Figure S17. The SEM graph of **NC-Ag6** (a) original, (b) crushed and (c) recrystallized.

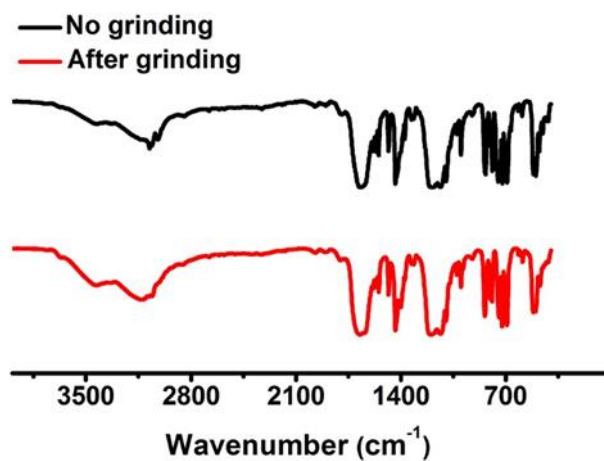


Figure S18. The FT-IR spectra of NC-Ag6 before and after grinding.

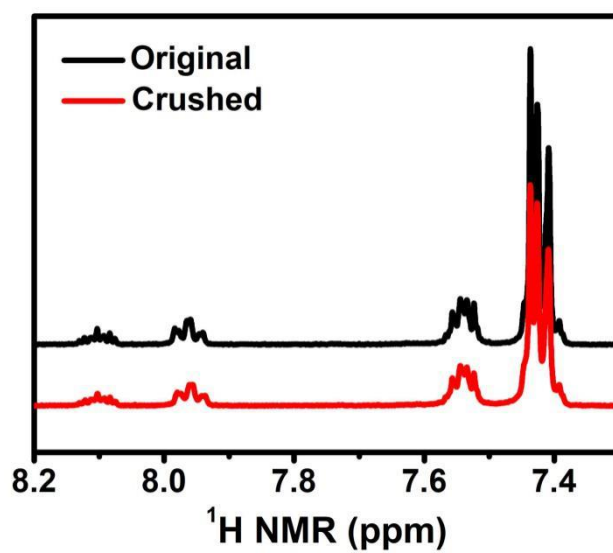


Figure S19 ¹H NMR spectra of original and crushed in dimethyl sulfoxide.

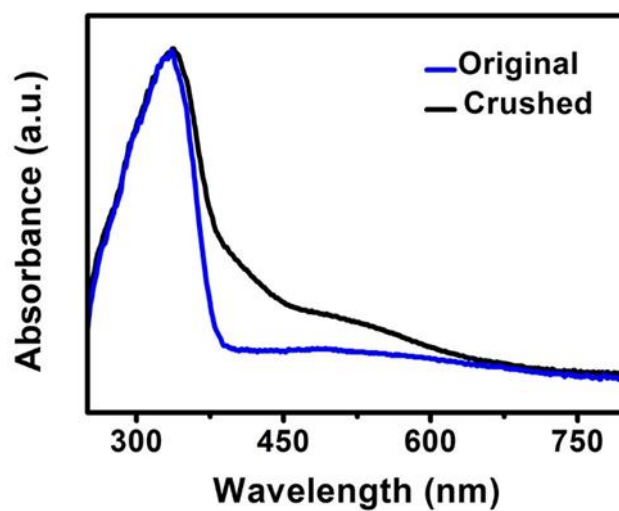


Figure S20. UV-vis diffuse reflectance spectra of NC-Ag6 before and after grinding in solid-state.

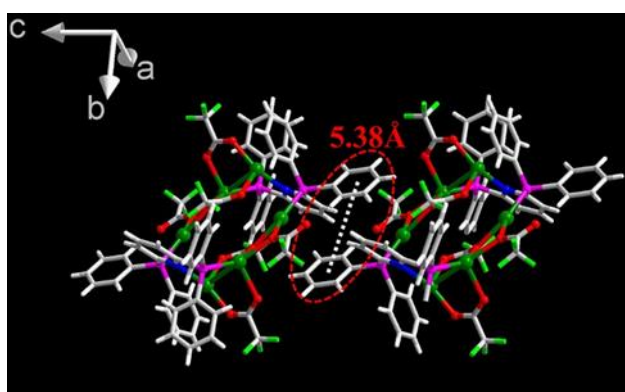


Figure S21. Two neighbouring NC-Ag6 molecular unit structures. The distance between the centers of the benzene ring is 5.38 Å

Table S5. Luminescence properties of **NC-Ag6** crushed (τ : emission lifetime, Φ : emission quantum yield).

	λ_{\max} (nm)	τ (μ s)	Φ (%)
NC-Ag6 crushed	493	18.1	20.22

Table S6 Temperature-dependent emission lifetime (τ) and corresponding fractional contributions (%) of solid-state **NC-Ag6** that after grinding excited at 355 nm, respectively (χ^3 : fitting parameter).

Temperature	χ^3	τ_1 (μ s) (%)	τ_2 (μ s) (%)	τ_3 (μ s) (%)	τ (μ s)
83K	1.16	310 (46.92)	90.5 (33.33)	1300 (19.75)	431.8
103K	1.12	300 (47.45)	90.3 (33.2)	1190 (19.35)	403.8
123K	1.16	315 (46.82)	98.1 (36.19)	1210 (16.99)	388.5
143K	1.16	87.3 (34.09)	267 (49.36)	1000 (16.55)	327.5
163K	1.12	81.9 (34.33)	238 (50.76)	863 (14.9)	277.3
183K	1.11	79.2 (40.99)	208 (48.22)	708 (10.79)	209.3
203K	1.16	68.6 (44.41)	168 (47.52)	537 (8.07)	153.5
223K	1.20	51.2 (35.08)	111 (55.69)	329 (9.23)	110.2
243K	1.24	38.5 (39.15)	88.9 (57.33)	311 (3.52)	77
263K	1.14	48.4 (73.33)	126 (12.48)	19.2 (14.19)	54
283K	1.24	533 (1.21)	53.3 (50.02)	21.7 (48.77)	43.7
293K	1.28	364 (2.15)	34.3 (64.99)	12.7 (32.86)	34.3

Tables of crystal data and structure refinements

Crystal data and structure refinement for NC-Ag6.

Identification code	NC-Ag6
CCDC number	1966339
Empirical formula	C ₃₆ H ₂₄ Ag ₃ Cl ₃ F ₉ NO ₆ P ₂
Formula weight	1229.46
Temperature/K	200.00(10)
Crystal system	monoclinic
Space group	<i>P</i> 2 ₁ / <i>n</i>
<i>a</i> /Å	12.39040(10)
<i>b</i> /Å	26.0236(2)
<i>c</i> /Å	13.09980(10)
α /°	90
β /°	94.1310(10)
γ /°	90
Volume/Å ³	4212.96(6)
<i>Z</i>	2
$\rho_{\text{calc}}/\text{cm}^3$	1.938
μ/mm^{-1}	14.319
<i>F</i> (000)	2392.0
Crystal size/mm ³	0.01 × 0.006 × 0.005
Radiation	CuK α (λ = 1.54184)
2 θ range for data collection/°	6.794 to 145.452
Index ranges	-14 ≤ <i>h</i> ≤ 15, -24 ≤ <i>k</i> ≤ 32, -16 ≤ <i>l</i> ≤ 16
Reflections collected	24591
Independent reflections	8179 [<i>R</i> _{int} = 0.0343, <i>R</i> _{sigma} = 0.0379]
Data/restraints/parameters	8179/12/595
Goodness-of-fit on <i>F</i> ²	1.029
Final <i>R</i> indexes [<i>I</i> ≥ 2 σ (<i>I</i>)]	<i>R</i> ₁ = 0.0365, <i>wR</i> ₂ = 0.0943
Final <i>R</i> indexes [all data]	<i>R</i> ₁ = 0.0410, <i>wR</i> ₂ = 0.0970
Largest diff. peak/hole / e Å ⁻³	1.61/-1.38

$$R_1 = \sum ||F_o| - |F_c|| / \sum |F_o|. \quad wR_2 = [\sum w(F_o^2 - F_c^2)^2 / \sum w(F_o^2)^2]^{1/2}$$

Supplementary References

- 1 CrysAlisPro 2012, Agilent Technologies. Version 1.171.36.31.
- 2 Sheldrick, G. M. A short history of SHELX. *Acta Cryst. A*, 2008, 64, 112.
- 3 Dolomanov, O. V., Bourhis, L. J., Gildea, R. J., Howard, J. A. K. & Puschmann, H. OLEX2: acomplete structure solution, refinement and analysis program. *J. Appl. Cryst.*, 2009, 42, 339.
- 4 Sheldrick, G. M. Crystal structure refinement with SHELXL. *Acta Cryst. C*, 2015, 71, 3.

- 5 Bootharaju, M. S.; Kozlov, S. M.; Cao, Z.; Harb, M.; Maity, N.; Shkurenko, A.; Parida, M. R.; Hedhili, M. N.; Eddaoudi, M.; Mohammed, O. F.; Bakr, O. M.; Cavallo, L.; Basset, J.-M. *J. Am. Chem. Soc.* 2017, 139, 1053–1056.
- 6 Döllefeld, H.; Weller, H.; Eychmüller, A. *J. Phys. Chem. B.* 2002, 106, 5604–5608.